Journal of Molecular Graphics and Modelling 51 (2014) 64–72

Contents lists available at ScienceDirect

Journal of Molecular Graphics and Modelling

journal homepage: www.elsevier.com/locate/JMGM

Group-based QSAR and molecular dynamics mechanistic analysis revealing the mode of action of novel piperidinone derived protein–protein inhibitors of p53-MDM2

Sukriti Goyal[a], Sonam Grover[b], Jaspreet Kaur Dhanjal[b], Chetna Tyagi[b], Manisha Goyal[a], Abhinav Grover[b,*]

[a] Apaji Institute of Mathematics & Applied Computer Technology, Banasthali University, Tonk 304022, Rajasthan, India
[b] School of Biotechnology, Jawaharlal Nehru University, New Delhi 110067, India

ARTICLE INFO

Article history:
Accepted 28 April 2014
Available online 4 May 2014

Keywords:
MDM2
p53
Cancer
QSAR
Piperidinone
Library

ABSTRACT

Tumour suppressor p53 is known to play a central role in prevention of tumour development, DNA repair, senescence and apoptosis which is in normal cells maintained by negative feedback regulator MDM2 (Murine Double Minute 2). In case of dysfunctioning of this regulatory loop, tumour development starts thus resulting in cancerous condition. Inhibition of p53-MDM2 binding would result in activation of the tumour suppressor. In this study, a novel robust fragment-based QSAR model has been developed for piperidinone derived compounds experimentally known to inhibit p53-MDM2 interaction. The QSAR model developed showed satisfactory statistical parameters for the experimentally reported dataset (r^2 = 0.9415, q^2 = 0.8958, pred_r^2 = 0.8894 and *F*-test = 112.7314), thus judging the robustness of the model. Low standard error values (r^2_se = 0.3003, q^2_se = 0.4009 and pred_r^2_se = 0.3315) confirmed the accuracy of the developed model. The regression equation obtained constituted three descriptors (R_2-DeltaEpsilonA, R_1-RotatableBondCount and R_2-SssOCount), two of which had positive contribution while third showed negative correlation. Based on the developed QSAR model, a combinatorial library was generated and activities of the compounds were predicted. These compounds were docked with MDM2 and two top scoring compounds with binding affinities of −10.13 and −9.80 kcal/mol were selected. The binding modes of actions of these complexes were analyzed using molecular dynamics simulations. Analysis of the developed fragment-based QSAR model revealed that addition of unsaturated electronegative groups at R_2 site and groups with more rotatable bonds at R_1 improved the inhibitory activity of these potent lead compounds. The detailed analysis carried out in this study provides a considerable basis for the design and development of novel piperidinone-based lead molecules against cancer and also provides mechanistic insights into their mode of actions.

1. Introduction

Cancer is a major health problem caused by unregulated growth and division of cells. Normal cells turn into cancerous cells due to many reasons, major one being mutations in the critical genes. According to the world cancer report, 12.7 million new cases diagnosed and reported in 2008 are expected to rise to 21 million by 2030 [1]. Better diagnosis as well as improving survival rates has played an important role in increasing number of cancer survivors. Side effects of the conventional treatment plans such as decrease in bone density, cardiovascular diseases, cognitive deficits, fatigue, physical and emotional distress, infertility and pulmonary dysfunction etc. in addition to drug resistance has posed a need for more effective and less toxic anticancer therapeutics [2,3].

As compared to conventional drug development methods, in silico methods are a good and viable alternative for identification and development of novel drug leads. One such in silico method is ligand-based drug design which establishes a quantitative structure-activity relationship (QSAR) between the inhibitory activity and structure of the inhibitors. Group-based QSAR (GQSAR) is a new fragment based method that allows studying the relationship of variation in the biological response with molecular fragments of interest by evaluating fragment-dependent

* Corresponding author. Tel.: +91 8130738032; fax: +91 11 26742040.
E-mail addresses: abhinavgr@gmail.com, agrover@mail.jnu.ac.in (A. Grover).

http://dx.doi.org/10.1016/j.jmgm.2014.04.015
1093-3263/

descriptors [4]. Unlike the conventional QSAR methods, GQSAR can be developed for both congeneric (template-based approach) as well as non-congeneric series (user-defined scheme) of compounds to obtain site specific clues, which has to be optimized for designing new molecules and quantitatively predicting their activity. This approach provides robust models in terms of the contribution of each individual substituent site that can be applied to create a combinatorial library by substituting different entities at these sites and then predicting their activities. This approach has been exploited in this study to develop novel piperidinone derived inhibitors with enhanced inhibitory effect on the basis of mathematical QSAR model.

New treatment methods aim at molecular targets such as oncogenes and tumour suppressors that are known to be involved in the progress of human cancers [5]. Tumour suppressor p53 is one such target which regulates the cell cycle, apoptosis, DNA repair, senescence and angiogenesis [6–8]. In normal cells, activity and concentration levels of p53 are regulated by MDM2 which is a ubiquitously expressed protein and plays an important role in tissue development. p53 and MDM2 mutually control their cellular levels by an autoregulatory feedback loop. When the level of MDM2 increases, it binds to p53 and inactivates it by directly blocking p53 transactivation domain. Dysfunction of this regulatory loop results in tumour formation. Thus, by inhibiting MDM2, p53 would fail to bind with MDM2 resulting in stabilization and activation of the tumour suppressor, ultimately leading to cell cycle arrest or programmed cell death (apoptosis) of cancer cells. Recently, cis-imidazoline derived MDM2 antagonists (nutlins) were identified in an in vivo study which focuses on activation of p53 tumour suppression pathway [9]. Drugs known to inhibit MDM2 were designed to block the hydrophobic cleft where three critical residues of p53 (Phe19, Trp23, Leu26) are known to bind, thus inhibiting the protein–protein interaction [9–12]. Based on the binding mode of already known inhibitors, a new series of piperidinone-derived compounds was identified experimentally which showed high inhibitory activity against p53-MDM2 interaction [13]. The binding affinity of these piperidinone-derived compounds for MDM2 improved through conformational change in both the piperidinone ring and the appended N-alkyl substituent.

In this study, we carried out fragment based QSAR study on a congeneric set of piperidinone derivatives. The aim of this study was to generate a reliable GQSAR model of piperidinone derived p53-MDM2 interaction inhibiting compounds which maps the variation of biological activity of the chosen compounds as a function of their site-specific molecular fragments. This model predicted the relationship between inhibitory activity and electronic and chemical properties of the derived compounds with high correlation. Our GQSAR model identified descriptors evaluated specifically for the fragments of piperidinone derivatives which are necessary for exhibiting anticancer activity. In addition to QSAR, we also provide detailed insights into the mode of binding of this class of compounds. In this study an attempt has been made to understand the effect of various substituents at two substitution sites in a common template derived from experimentally reported dataset by predicting the inhibitory activity of synthesized combinatorial library of piperidinone derived molecules and then virtually docking it with MDM2. After molecular dynamics simulations of the ligand bound protein complexes, ADME properties of these ligands were predicted for further analysis. This analysis would help in providing novel piperidinone-based lead molecules for the development of anticancer drugs. This study will enhance understanding and provide insight into mechanism of action of piperidinone derivatives as potent anticancer therapeutics in terms of structural requirements needed for drug development.

2. Materials and methods

2.1. Selection and preparation of data set

A dataset of 23 previously reported piperidinone-derived compounds [13] was drawn using MarvinSketch [14]. The 2D compounds were converted into 3D using VlifeEngine module of VLifeMDS ver.4.3 [15]. These 3D compounds were energy minimized using force field batch minimization module of VlifeEngine and then used for developing the GQSAR model.

2.2. Calculation of descriptors for GQSAR model

The GQSAR module of VLifeMDS was used for building fragment based QSAR model. Using modify utility of VLifeMDS, a template for the congeneric set of piperidinone derived compounds was created by keeping a common moiety and substituting groups at the two sites (named R_1 and R_2) of substitution. The optimized set of compounds and the template created were selected for fragment-based GQSAR model building. The inhibitory activity values of the molecules in the form of pIC_{50} were manually incorporated in VLife MDS platform and the physico-chemical 2D descriptors were calculated for different substituents present at both substitution sites (i.e. at fragments R_1 and R_2) of the dataset molecules (Supplementary Table 1). Since the same descriptors were calculated for various groups at two different sites, a particular nomenclature was applied for naming a descriptor at a particular position. For example R_1_RotatableBondCount signifies the number of rotatable bonds at R_1 substitution site. Invariable columns were removed leaving a total of 174 from 343 descriptors for QSAR analysis. The training and test sets were selected manually keeping a uniform distribution of compounds in the two sets based on their pIC_{50} values. Six molecules, namely 7, 8, 14, 15, 18 and 20 were chosen as test set, while the remaining 17 were selected as training set. The unicolumn statistics of the selected training and test sets were calculated and analyzed.

Supplementary Table 1 related to this article can be found, in the online version, at http://dx.doi.org/10.1016/j.jmgm.2014.04.015.

2.3. Building the GQSAR model of piperidinone-derived compounds

For this study, out of various model building methods stepwise forward partial least square regression method was implemented. The stepwise forward variable selection algorithm began by developing a trial model one step at a time with only one independent variable. At each step independent variables were added one by one and then the fitness of the model was evaluated using the PLS (partial least square) cross-validation method. Accordingly, the model was constantly changed from the previous one by adding or removing a predictor variable. This method continued until there are no more significant variables left outside the model. The advanced variable selection and model building wizard was utilized for this purpose with cross correlation limit as 0.7, *F*-test as 4, term selection criteria as r^2, variance cut-off as 0.1 and number of random iterations as 100.

2.4. Validation of the developed GQSAR model

The 'goodness of fit' of the developed model was analyzed using different statistical parameters, such as r^2, q^2, pred_r^2, *F*-test and standard error [16]. A model is considered to be robust when it fulfils the conditions: $r^2 > 0.6$, $q^2 > 0.6$ and pred_$r^2 > 0.5$ [16,17]. The *F*-test denotes the ratio of the variance observed by the model and the variance due to error in regression. High *F*-test value indicates that the model is statistically significant which shows a negligible

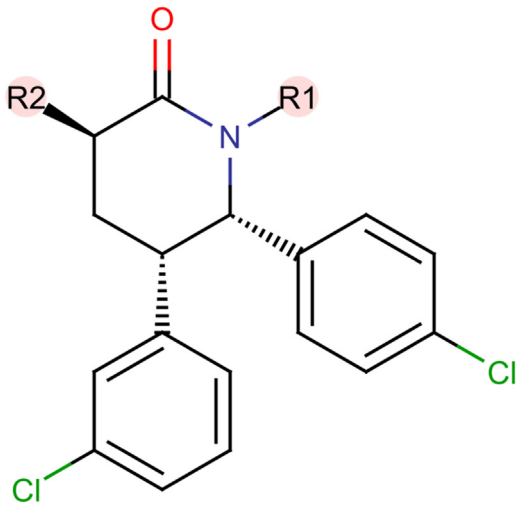

Fig. 1. Structure of common template of piperidinone derived compounds.

probability of failure of the developed model. The low standard error (Pred_r^2se, q^2_se and r^2_se) shows absolute quality of fitness of the model.

2.5. Cross-validation of the model

Internal validation of the QSAR model developed was carried out using leave-one-out (q^2, LOO) method [18]. Cross-validated correlation coefficient, q^2, was calculated by sequentially removing each compound in the training set, refitting the model using the same descriptors, and predicting the biological activity of the removed molecule using the refit model. The formula used for calculating q^2 was

$$q^2 = 1 - \frac{\sum (y_i - \hat{y}_i)^2}{\sum (y_i - y_{\text{mean}})^2}$$

where y_i and $\hat{y}_i$ are the actual and predicted activities of the ith molecule in the training set respectively and y_{mean} is the average activity of all the molecules in the training set. External validation of the model was performed by predicting the activity of each molecule in the test set using the model generated from the training set. The pred_value was calculated using the following formula:

$$\text{pred\_}r^2 = 1 - \frac{\sum (y_i - \hat{y}_i)^2}{\sum (y_i - y_{\text{mean}})^2}$$

where y_i and $\hat{y}_i$ are the actual and predicted activities of the ith molecule in the test set respectively and y_{mean} is the average activity of all molecules in the training set. Y randomization test was used for checking the robustness of the chosen model. The robustness of the models for training sets was examined by comparing these models to those derived for random data sets. Random sets of test and training set were generated by rearranging the molecules and their activities in the training set. The significance of the

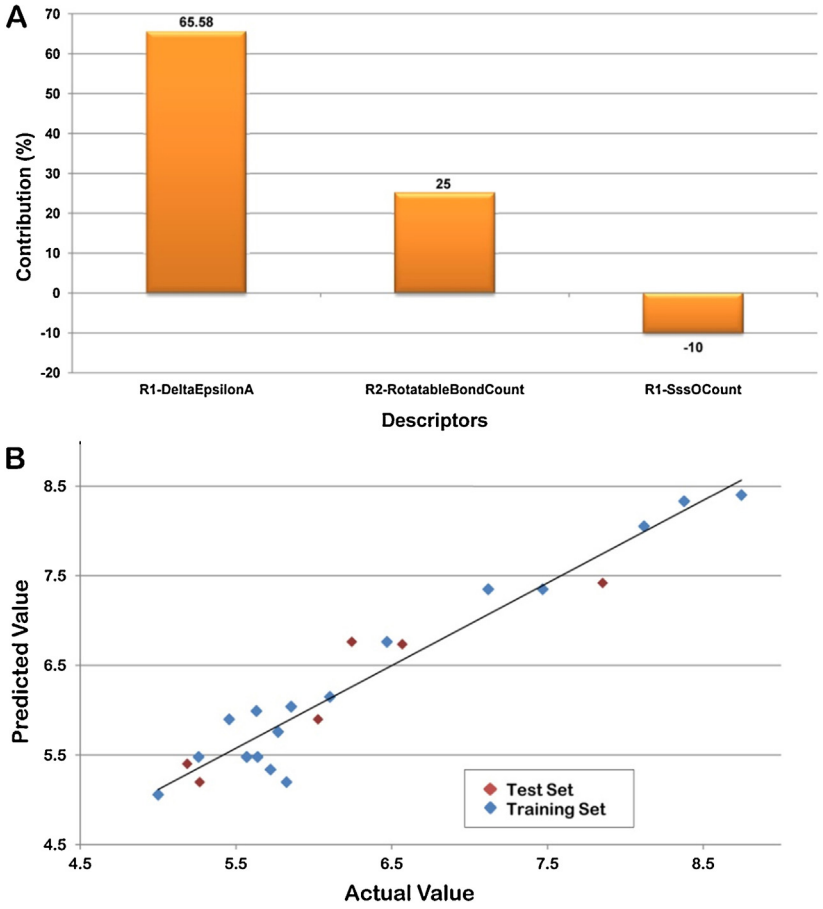

Fig. 2. (a) Contribution plot of the three descriptors of the developed GQSAR model. (b) Graphical representation of observed vs. predicted activity for training and test set.

models thus obtained was based on a calculated *Z*-score. A *Z*-score value was calculated as follows:

$$Z_{\text{score}} = \frac{(h - \mu)}{\sigma}$$

where h is the q^2 value calculated for the actual data set, μ the average q^2 and σ is its standard deviation calculated for various iterations using models built from different random data sets.

2.6. Generation of combinatorial library based on GQSAR model

Combinatorial library was created using the Leadgrow module of VLifeMDS by substituting different groups at the two substitution sites – R_1 and R_2. One library was created by substituting some selective atoms, alkyl groups, rings (including aromatic rings) and charged groups at both R_1 and R_2 position. The library consisted of around 28,000 compounds. The validated GQSAR model was then used to predict the activity of the compounds of this library.

2.7. Docking of top scoring compounds with MDM2

The docking of compounds on to the target MDM2 was carried out using the Glide module of Schrodinger [19]. The protein was first prepared using protein preparation wizard of Glide, which involved removal of water molecules, capping of termini, adding explicit hydrogen atoms, treating disulphides and finding overlaps. The prepared protein was then optimized and used for creation of a grid around the interacting residues by receptor grid generation platform of Schrodinger.

The structures of combinatorial library compounds with high predicted activity values were cleaned using MarvinSketch and their conformations were prepared using LigPrep module of Maestro interface. These ligands were docked against MDM2 using extra precision GlideXP platform and were ranked based on their binding affinities. The top two compounds were merged with the protein separately and the complexes were analyzed. For gaining better insight into their binding modes, the most active compound of the experimentally derived piperidinone series was docked with MDM2.

Table 1
Unicolumn statistics for training and test sets for MDM2-p53 inhibitory activity.

Data set	Average	Max	Min	Std dev	Sum
Training set	6.3598	8.7440	5.0000	1.1616	108.1170
Test set	6.1915	7.8540	5.1870	0.9796	37.1490

2.8. Molecular dynamics simulations

The coordinates of the ligand-bound protein complex were optimized in the protein preparation wizard (Schrodinger) where hydrogens were added; water molecules, UDP and peptide were removed, and the complex structure was minimized using the OPLS2001 forcefield. The 1-μm simulation used the CHARM27 forcefield [20], and the simple point charge model for water. The CHARM27 forcefield was applied to the system using the VIPARR utility. The default Desmond relaxation was performed before simulation, and molecular dynamics were run at constant temperature (300 K) and pressure (1 bar). The simulation was performed by using the programme Desmond [21].

3. Results and discussion

3.1. Separation of data set into training and test sets

The chosen 23 compounds were divided into the training and the test set, where training set contained 17 while the test set contained 6 compounds. The unicolumn statistics was calculated for the training and test set as shown in Table 1. The sets were validated by confirming that the highest value of the test set was less than or equal to highest of training set and the lowest value of the test set was greater than or equal to lowest of training set, i.e., the test set lied in the range of the training set. The values calculated thus confirmed that the test set was interpolative and was derived within the min–max range of the training set. The mean and standard deviation of the training and test set provided an idea of the relative deviation of mean and point density distribution (along mean) of the two sets.

Table 2
Contribution of physico-chemical descriptors and predicted activity values.

Compound No.	R_2-DeltaEpsilonA	R_1-RotatableBondCount	R_2-SssOCount	Prediction (pIC_{50})
1	0.258	1	0	7.35
2	0	0	0	5.058
3	0	1	0	5.198
4	0	2	0	5.338
5	0	3	0	5.479
6	0	3	0	5.479
7	0	1	0	5.198
8	0	6	0	5.899
9	0	6	0	5.899
10	0	7	0	6.04
11	0	5	0	5.759
12	0	3	0	5.479
13	0.258	1	0	7.35
14	0.024	1	0	5.4
15	0.188	1	0	6.763
16	0.188	1	0	6.763
17	0.188	1	1	6.149
18	0.184	1	0	6.734
19	0.095	1	0	5.991
20	0.267	1	0	7.42
21	0.258	6	0	8.052
22	0.258	8	0	8.332
23	0.267	8	0	8.402

Table 3
Predicted activity of various substituted groups at R_1 and R_2 for the combinatorial library.

S. No.	R_1	R_2				
		Flourine	Carboxylate	Carbonic	Carboxyl	Chlorine
1 2 3	Butyl Isobutyl Tert-butyl	10.12	9.92	9.68	8.89	8.92
4 5 6 7	Isopropyl Acetate Carbonic Carbomethoxy	9.98	9.78	9.54	8.75	8.78
8 9 10 11 12 13	Ethyl Allyl Carboxyl Methyl-ketone Benzyl Phenoxy	9.84	9.64	9.402	8.61	8.64

3.2. Analysis of fragment based QSAR model of piperidinone-derived compounds

In this study, we developed a robust fragment-based QSAR model to evaluate the correlation between the physico-chemical descriptors and contribution of each individual substitution site of piperidinone derivatives using a common template (Fig. 1). Among all the GQSAR models, the best one was selected considering various statistical parameters such as correlation coefficient ($r^2 > 0.6$), cross-validated correlation coefficient ($q^2 > 0.6$), predicted correlation coefficient (pred_$r^2 > 0.5$), and *F*-test values at 99% significance level. The model chosen on the basis of all these parameters was:

$$\begin{aligned} \text{pIC50} &= (8.3382 \times \text{R}_2 - \text{DeltaEpsilonA}) \\ &\quad + (0.1402 \times \text{R}_1 - \text{RotatableBONdCount}) \\ &\quad - (0.6180 \times \text{R}_2 - \text{SssoCount}) + 5.0581 \end{aligned}$$

$$n = 17, \text{degreeoffreedom} = 14, r^2 = 0.9415, q^2 = 0.8958,$$

$$F\text{-test} = 112.7314, r^2\_\text{se} = 0.3003,$$

$$q^2\_\text{se} = 0.4009, \text{pred}\_r^2 = 0.8894, \text{pred}\_r^2\text{se} = 0.3315$$

where '*n*' is the number of compounds in regression, 'r^2' is squared correlation co-efficient indicating relative measure of quality of fit, '*F*-test' (Fischer's value) denoting chance statistics assuring that the results are not merely based on chance correlations, '$q^{2'}$ is cross-validated squared correlation coefficient and pred_r^2 is predicted squared correlation coefficient. The GQSAR model on the basis of stepwise forward algorithm selected three physico-chemical descriptors out of 174 namely, R_2-DeltaEpsilonA, R_1-RotatableBondCount and R_2-SssOCount.

R_2-DeltaEpsilonA is a descriptor from the class extra topochemical indices. It shows the contribution of electronegativity and unsaturation at the substitution site. It is defined as the difference of measure of electronegative atom count and measure of electronegative atom count in alkane (reference molecule). Electronegative atom has a tendency to attract electrons towards itself. It has a positive contribution of about 65%, which can be seen in the contribution plot (Fig. 2a), indicating that the presence of unsaturation and an electronegative entity in the compound would enhance the inhibitory efficiency of the novel lead compound. The second descriptor, R_1-RotatableBondCount describes the number of rotatable bonds at R_1 substitution site. Rotatable bonds are defined as any single bond bound to a non-terminal heavy (i.e., non-hydrogen) atom. The positive sign associated with this descriptor in the GQSAR model indicates that increase in the rotatable bonds, i.e., saturated single bonds in the molecule is advantageous for MDM2 binding property exhibited by all the compounds. The third and final descriptor, R_2-SssOCount is a type of physicochemical descriptor belonging to the class Estate Numbers and is defined as the total number of oxygen connected with two single bonds. It shows a negative correlation with biological activity signifying that presence of oxygen atom bonded with two single bonds would result in decrease of the compound's inhibitory activity.

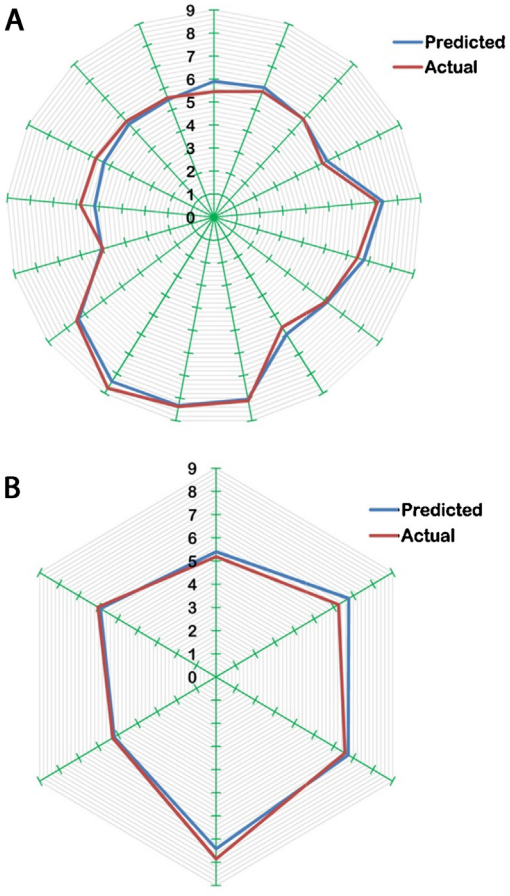

Fig. 3. Radar plots showing alignment of (a) observed and predicted activity values for training set, (b) observed and predicted activity value for test set.

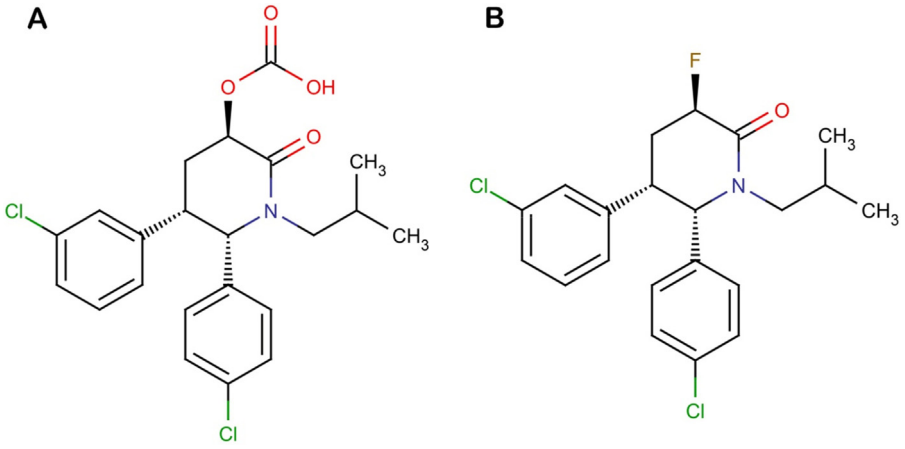

Fig. 4. Chemical structures of designed two highly active compounds. (a) R_1 – isobutyl, R_2 – carbonic. (b) R_1 – isobutyl, R_2 – flourine.

The contribution of these three descriptors along with the predicted pIC_{50} values of the dataset compounds is mentioned in Table 2. Minimal difference between the experimental activity values and the predicted activity values depicts the high quality of the QSAR model, which can thus be used for predicting activity values of compounds of combinatorial library. Significance of the QSAR model can be judged from various statistical parameters. The developed model showed a high correlation coefficient of 0.9415 along with a low standard error of 0.3003, thus depicting the accuracy of the model. High value of *F*-test (112.7314) suggested the statistical robustness of the G-QSAR model thus indicating that the probability of failure for this model is very low. The cross-validated correlation coefficient q^2 calculated by Leave-One-Out method had a value of 0.8958 which showed a good internal prediction power of the developed model while a good external predictive potential was judged by a high value of pred_r^2 (in this case 0.8894). A plot of observed vs. predicted inhibitory activity and radar graphs of the actual and predicted inhibitory activity for training and test set is shown in Figs. 2b and 3 respectively. Low standard error values were indicative of the absolute quality of the generated model. Thus, it can be said that the developed GQSAR model was robust, reliable and predictive.

An analysis of the results above showed that substitution of electronegative and unsaturated groups at R_2 position enhances the inhibitory activity of the potential lead compound while at R_1 position saturated or single bonds increases the inhibitory power of the potent lead compound and oxygen atom with two single bonds at R_2 decreases the same.

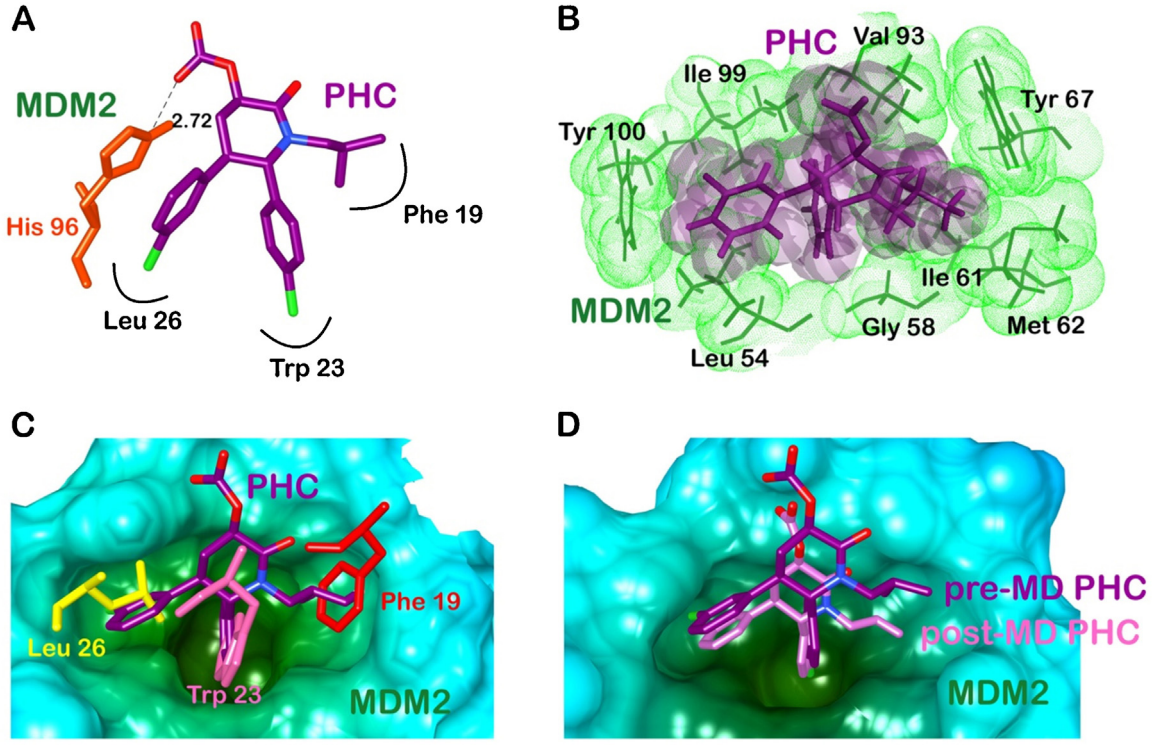

Fig. 5. Molecular interactions of MDM2 with designed compound PHC (purple): (a) depiction of hydrogen bond with His96 (MDM2) (orange); (b) hydrophobic interaction (green); (c) superposition of three critical residues of p53 (Phe19 – red, Trp23 – pink, Leu26 – yellow) and PHC occupying the hydrophobic clefts; (d) superposition of pre- and post-MD simulations complexes.

Table 4
Glide scores and its various components.

Complex	PHC-MDM2	FPO-MDM2	TBB-MDM2
GScore	−10.12	−9.8	−8.19
Hbond	−1.6	−0.64	0
E_{vdw}	−41.25	−38.92	−52.07
E_{coul}	−5.79	−0.25	−4.67
Emodel	−60.64	−55.15	−77.88
Energy	−47.04	−39.18	−56.74
Ligand strain energy	4.92	2.96	0.78

3.3. Prediction and analysis of combinatorial library generated on the basis of developed GQSAR model

A combinatorial library was created by substituting atoms, alkyl groups, rings (including aromatic rings) and charged groups at both the substitution sites R_1 and R_2. The developed GQSAR model was used for predicting the inhibitory activity values of the compounds generated. The predicted activity values (pIC50) of the combinatorial library compounds are listed in Table 3.

A total of 28,000 compounds were generated and their predicted activity ranged from 10.12 to −61.595 out of which 524 compounds had a predicted activity above the highest inhibitory activity of the experimentally reported inhibitors, i.e., 8.74. Analysis of these compounds revealed that presence of four specific groups at R_2 had a positive effect on the inhibitory power and presence of rotatable bonds at R_1 enhanced it further. The groups responsible for improved inhibitory activity are fluorine, carbonic, carboxylate and chlorine at R_2 position and butyl, isobutyl, tert-butyl, isopropyl, acetate, carbonic, carbomethoxy, ethyl, allyl, carboxyl, methyl-ketone, benzyl and phenoxy at R_1 position. The groups positioned at R_1 had rotatable bonds thus improving the inhibitory activity, with highest number in isobutyl. Presence of oxygen atoms with single bonds resulted in decreased inhibitory action due to a negatively correlated descriptor R_2-SssOCount. While the above mentioned compounds enhanced the therapeutic effect, elements such as phosphorous, boron, potassium and silicon among others diminished the same, resulting in inactive compounds.

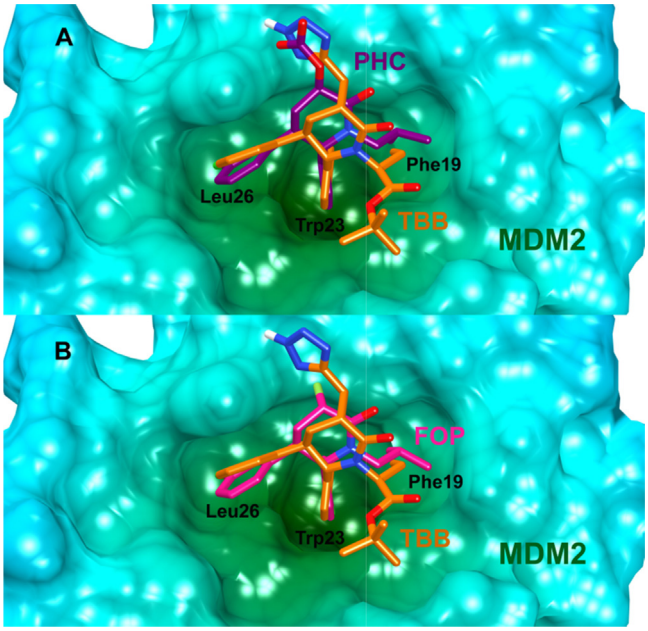

Fig. 6. Superposition of TBB with (a) PHC and (b) FPO.

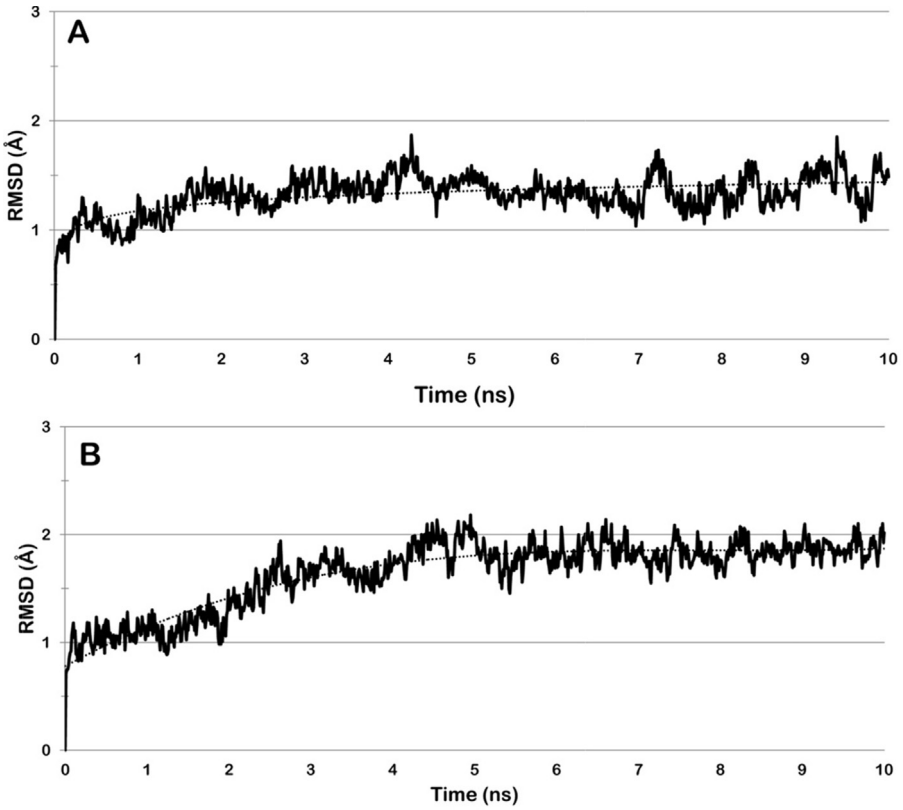

Fig. 7. RMSD plot of MD simulations: (a) PHC bound MDM2 complex and (b) FPO bound MDM2 complex.

3.4. Mechanistic analysis and mode of action of the compounds screened from the combinatorial library

The top scoring compounds with predicted activity greater than the highest inhibitory activity of experimentally reported compounds were docked against MDM2 [PDB: 4JWR] [22]. Based on the Glide score, the two top scoring compounds were selected and their interactions were analyzed. The first compound, *5-(3-chlorophenyl)-6-(4-chlorophenyl)-1-(2-methylpropyl)-2-oxopiperidin-3-yl hydrogen carbonate* (PHC) (Fig. 4a), containing isobutyl group at R_1 and carbonic at R_2 displayed a high binding score of −10.13 kcal/mol. The second compound, *(3R, 5S, 6S)-5-(3-chlorophenyl)-6-(4-chlorophenyl)-3-fluoro-1-(2-methylpropyl)piperidin-2-one* (FPO) (Fig. 4b), substituted with isobutyl group at R_1 and fluorine atom at R_2 position, possessed a binding score of −9.80 kcal/mol. The breakdown of the Glide score of the two compounds into their various components is mentioned in Table 4. The compounds occupied the three hydrophobic clefts of MDM2, which are otherwise utilized by the critical residues of p53 (Phe19, Trp23 and Leu26) when interacting with MDM2. Binding of the designed compounds to the hydrophobic cleft would result in disruption/dissociation of p53 binding to MDM2, resulting in activation of the tumour suppressor. The most active compound of the experimentally reported piperidinone series (pIC50 = 8.745), *tert-butyl(2S)-2-[(2S, 3R, 5R)-3-(3-chlorophenyl)-2-(4-chlorophenyl)-6-oxo-5-(1H-1, 2, 3, 4-tetrazol-5-ylmethyl)piperidin-1-yl]butanoate* (TBB), was also docked with MDM2. It exhibited a binding score of −8.19 kcal/mol, which is less than that of PHC (−10.13 kcal/mol) and FPO (−9.80 kcal/mol). Higher binding score of PHC and FPO than TBB indicated improved binding affinities of the two designed compounds.

3.5. PHC, carbonic group substituted compound against p53-MDM2 interaction

This compound exhibited a glide score of −10.13 kcal/mol and a predicted activity of 9.68. Analysis of the PHC docked MDM2 complex revealed one hydrogen bond interaction and numerous hydrophobic contacts between the protein and the ligand. The hydrogen bond (2.72 Å) was formed between oxygen atom of carbonic group of PHC and second epsilon nitrogen of histidine (Fig. 5a). The MDM2 residues involved in hydrophobic interactions with PHC were Leu54, Gly58, Ile61, Met62, Tyr67, Val93, Ile99 and Tyr100 as shown in Fig. 5b. As mentioned by Rew et al. [22, p. 6], the two chlorophenyl rings of piperidinone derived inhibitors occupied the hydrophobic clefts which are otherwise occupied by Leu26 and Trp23 of p53. The analysis of the PHC and MDM2 interaction were in accordance with the observations made by Rew et al. Hydrogen bond provided stability to the ligand-bound structure whereas hydrophobic interactions mimicked p53 binding to MDM2 (Fig. 5c). Chlorophenyl positioned at the second position of piperidinone ring occupied the Trp23 (p53) hydrophobic cleft, chlorophenyl substituted at fourth position occupied Leu26 (p53) cleft and isobutyl interacted with Phe19 (p53) cleft. TBB was also observed to be occupying the same hydrophobic cleft as PHC as shown in Fig. 6a.

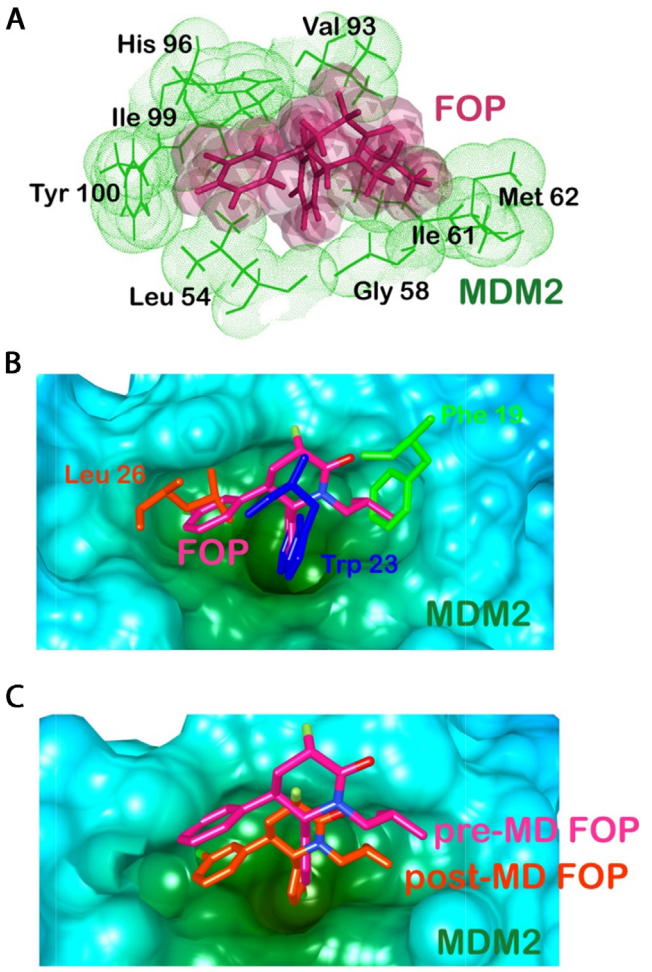

Fig. 8. Molecular interactions of MDM2 with designed compound FOP (pink): (a) depiction of hydrophobic interaction (green); (b) superposition of three critical residues of p53 (Phe19 – green, Trp23 – blue, Leu26 – orange) and FOP occupying the hydrophobic clefts; (c) superposition of pre- and post-MD simulations complexes. (For interpretation of the references to colour in this figure legend, the reader is referred to the web version of this article.)

MD simulations of the PHC docked MDM2 complex resulted in a more energetically stable ligand bound protein complex with ligand PHC moving further into the hydrophobic cleft while losing the sole hydrogen bond interaction as shown in Fig. 5d. The energy minimized complex displayed stability from 2 to 10 ns (Fig. 7a). Thus, post MD simulations all interacting residues were involved in hydrophobic interactions.

3.6. FPO, fluorine substituted compound against p53-MDM2 interaction

FPO has an isobutyl group positioned at R_1 position while fluorine is substituted at R_2 position. It possessed a docking score of −9.80 kcal/mol and predicted inhibitory activity of 10.12. Since, fluorine is the most electronegative element known it had the highest

Table 5
MDM2 residues involved in molecular interaction with PHC and FPO.

S. No.	Complex		Hydrogen bond	Hydrophobic
1	PHC-MDM2	Pre-MD	His96	Leu54, Gly58, Ile61, Met62, Tyr67, Val93, Ile99, Tyr100
		Post-MD	–	Leu54, Leu57, Gly58, Ile61, His73, Val 75, Phe91, Val93, Lys94, His96, Ile99
2	FPO-MDM2	Pre-MD	–	Leu54, Gly58, Ile61, Met62, Val93, His96, Ile99, Tyr100
		Post-MD	–	Gln24, Leu54, Leu57, Gly58, Ile61, His73, Phe91, Val93, His96, Ile99

predicted activity. As shown in Fig. 8a, FPO exhibited hydrophobic interactions with Leu54, Gly58, Ile61, Met62, Val93, His96 and Tyr100 residues of MDM2. FPO like PHC consisted of isobutyl group at R_1 thus utilizing the hydrophobic clefts of MDM2 in the same way as TBB (Fig. 6b) and PHC (Fig. 8b).

MD simulations of FPO docked MDM2 complex revealed a more energetically stable conformation with FPO moving further into the cavity. Analysis of the energy stabilized complex showed a stable complex from 4 to 10 ns with deviation under 2 Å (Fig. 7b). Post MD simulations the ligand was involved with hydrophobic interactions only (Fig. 8c). A summary of hydrogen bond and hydrophobic interactions formed by the ligands with MDM2 before and after MD simulations is provided in Table 5.

4. Conclusions

In the present study, a novel fragment-based QSAR model was developed for 23 piperidinone derived compounds as anticancer agents which have been reported to inhibit the p53-MDM2 interactions. The IC_{50} values were collected from literature and dataset was divided into training and test sets. The statistical parameters such as correlation coefficient r^2, cross-validated correlation coefficient q^2, predicted correlation coefficient pred_r^2, *F*-test and standard error fulfilled the conditions for a model to be considered robust. The QSAR equation obtained constituted three physico-chemical descriptors, namely R_2-DeltaEpsilonA, R_1-RotatableBondCount and R_2-SssOCount. The first two descriptors displayed positive contribution while the last one laid a negative correlation with the activity. A combinatorial library was created and activities of the compounds were predicted using the developed G-QSAR model. Analysis of the library revealed that substitution of unsaturated electronegative groups at R_2 and presence of rotatable bonds at R_1 enhanced the inhibitory activity of the compound while occurrence of an oxygen atom connected with two single bonds reduced the same. Thus positioning of groups such as butyl, isobutyl, tert-butyl, isopropyl, acetate, carbonic, carbomethoxy, ethyl, allyl, carboxyl, methyl-ketone, benzyl and phenoxy at R_1 position and fluorine, carbonic, carboxylate and chlorine at R_2 significantly improved the inhibitory effect of the compounds. Docking of the two top scoring compounds PHC and FPO with MDM2 revealed high binding affinities of these compounds in the p53 binding region of MDM2. These molecules can be considered as potent lead compounds against cancer as they will lead to disruption/dissociation of p53 binding to MDM2, thus activating the tumour suppressor p53. The methodology described here makes use of novel group based QSAR method as a useful tool in optimizing potent lead molecules. The traditional QSAR methodology considers the entire dataset molecule, whereas the GQSAR described here extracts the properties of the substituents alone and hence is more sensitive in identifying relationships and trends at specific functional sites of the molecules.

Conflicts of interest

The authors declare that they have no conflicts of interest.

Acknowledgements

AG is thankful to Jawaharlal Nehru University for usage of all computational facilities. AG is grateful to University Grants Commission, India for the Faculty Recharge Position.

References

[1] B. Peter, L. Bernard, World Cancer Report, WHO, 2008.
[2] R. Siegel, D. Naishadham, A. Jemal, Cancer statistics, CA. Cancer J. Clin. 62 (2012) 10–29.
[3] M.M. Gottesman, Mechanisms of cancer drug resistance, Annu. Rev. Med. 53 (2002) 615–627.
[4] S. Ajmani, K. Jadhav, S.A. Kulkarni, Group-based QSAR (G-QSAR): mitigating interpretation challenges in QSAR, QSAR Comb. Sci. 28 (2009) 36–51.
[5] M. Barinaga, Designing therapies that target tumor blood vessels, Science 275 (1997) 482–484.
[6] F. Toledo, C.J. Lee, K.A. Krummel, L.-W. Rodewald, C.-W. Liu, G.M. Wahl, Mouse mutants reveal that putative protein interaction sites in the p53 proline-rich domain are dispensable for tumor suppression, Mol. Cell. Biol. 27 (2007) 1425–1432.
[7] J.S. Fridman, S.W. Lowe, Control of apoptosis by p53, Oncogene 22 (2003) 9030–9040.
[8] K.H. Vousden, X. Lu, Live or let die: the cell's response to p53, Nat. Rev. Cancer 2 (2002) 594–604.
[9] L.T. Vassilev, B.T. Vu, B. Graves, D. Carvajal, F. Podlaski, Z. Filipovic, N. Kong, U. Kammlott, C. Lukacs, C. Klein, In vivo activation of the p53 pathway by small-molecule antagonists of MDM2, Sci. Signal. 303 (2004) 844.
[10] J.G. Allen, M.P. Bourbeau, G.E. Wohlhieter, M.D. Bartberger, K. Michelsen, R. Hungate, R.C. Gadwood, R.D. Gaston, B. Evans, L.W. Mann, Discovery and optimization of chromenotriazolopyrimidines as potent inhibitors of the mouse double minute 2-tumor protein 53 protein–protein interaction, J. Med. Chem. 52 (2009) 7044–7053.
[11] H.P. Beck, M. DeGraffenreid, B. Fox, J.G. Allen, Y. Rew, S. Schneider, A.Y. Saiki, D. Yu, J.D. Oliner, K. Salyers, Improvement of the synthesis and pharmacokinetic properties of chromenotriazolopyrimidine MDM2-p53 protein–protein inhibitors, Bioorg. Med. Chem. Lett. 21 (2011) 2752–2755.
[12] P.H. Kussie, S. Gorina, V. Marechal, B. Elenbaas, J. Moreau, A.J. Levine, N.P. Pavletich, Structure of the MDM2 oncoprotein bound to the p53 tumor suppressor transactivation domain, Science 274 (1996) 948–953.
[13] Y. Rew, D. Sun, F. Gonzalez-Lopez De Turiso, M.D. Bartberger, H.P. Beck, J. Canon, A. Chen, D. Chow, J. Deignan, B.M. Fox, Structure-based design of novel inhibitors of the MDM2-p53 interaction, J. Med. Chem. 55 (2012) 4936–4954.
[14] P. Csizmadia, MarvinSketch and MarvinView: molecule applets for the World Wide Web, in: Proceedings of ECSOC-3, the Third International Electronic Conference on Synthetic Organic Chemistry, 1999, pp. 367–369.
[15] Vlife MDS, Software Package, Version 3.0, Vlifescience Technologies Pvt. Ltd., Pune, 2008.
[16] A. Golbraikh, A. Tropsha, Beware of q2!, J. Mol. Graphics Modell. 20 (2002) 269–276.
[17] A. Afantitis, G. Melagraki, H. Sarimveis, O. Igglessi-Markopoulou, G. Kollias, A novel QSAR model for predicting the inhibition of CXCR3 receptor by 4-N-aryl-[14] diazepane ureas, Eur. J. Med. Chem. 44 (2009) 877–884.
[18] S. Izrailev, D. Agrafiotis, A novel method for building regression tree models for QSAR based on artificial ant colony systems, J. Chem. Inf. Comput. Sci. 41 (2001) 176–180.
[19] L. Schrödinger, Schrodinger suite, Maestro Version 8, 2008.
[20] N. Foloppe, A.D. MacKerell Jr., All-atom empirical force field for nucleic acids: I. Parameter optimization based on small molecule and condensed phase macromolecular target data, J. Comput. Chem. 21 (2000) 86–104.
[21] Schrodinger, Schrodinger Suite, Maestro LLC, New York, NY, 2009.
[22] F. Gonzalez-Lopez de Turiso, D. Sun, Y. Rew, M.D. Bartberger, H.P. Beck, J. Canon, A. Chen, D. Chow, T.L. Correll, X. Huang, Rational design and binding mode duality of MDM2-p53 inhibitorsJ, Med. Chem. 56 (2013) 4053–4070.